A new method to demonstrate frustrated total internal reflection in the visible band

Yizhuang You[a] and Xiaohan Wang
Kuang Yaming Honored School, Nanjing University, Nanjing, China 210089

Sihui Wang, Yonghua Pan, and Jin Zhou
Department of Physics, Nanjing University, Nanjing, China 210093

(Received 14 April 2007; accepted 22 November 2007)

We describe a new method to demonstrate frustrated total internal reflection in the visible band using the 100 nm thick air film near the center of Newton's rings. Experimental measurements of the light intensity distribution validate the theoretical predictions. © *2008 American Association of Physics Teachers.*

[DOI: 10.1119/1.2825389]

I. INTRODUCTION

Total reflection occurs when light travels from a medium with refractive index n to an optically less dense medium with refractive index n_0 at an incident angle equal to or greater than the critical angle $\theta_c = \arcsin(n_0/n)$. Besides being totally reflected, the incoming light penetrates into the less dense medium as an evanescent wave and travels for some distance parallel to the interface before being scattered back to the denser medium. If a third medium of refractive index n (that is, made of the same material as the first medium) is placed at a small distance d (of the same order of magnitude as the light wavelength) to the first medium, the incident light can travel partly through the middle medium into the third medium, and the reflected light in the first medium is weakened. This intriguing phenomenon is termed frustrated total internal reflection. A detailed review of theoretical and experimental studies on frustrated total internal reflection up to the 1980s is given in Ref. 1. The invention of the near-field scanning optical microscope in the 1980s[2–4] advanced the study of frustrated total internal reflection and led to a new branch of optics: near field optics.[5]

Although frustrated total internal reflection was originally introduced in optics and electrodynamics,[6] it is frequently described by books on quantum mechanics as "optical tunneling" to illustrate the barrier tunneling effect.[7] A demonstration of frustrated total internal reflection would help students better understand light propagation at interfaces and the phenomenon of tunneling.

Many experiments have been done to study frustrated total internal reflection. Some early experiments were conducted by Bose[8] and Hall[9] in the microwave band, so that the thickness of the middle medium was easy to control due to the long wavelength (several centimeters) of microwaves. But this kind of experiment is not quite as intuitive for students because the microwave beam cannot be directly seen. To show the phenomenon visually, it would be better to do experiments in the visible band.

One difficulty in realizing frustrated total internal reflection in the visible band is due to the relatively short wavelength (several hundred nanometers) of visible light. In 1966, Coon[10] quantitatively verified the theoretical prediction of frustrated total internal reflection in the visible band using the 546.1 nm Hg line. The experiment used a double prism arrangement and the gap between the prisms was a factor of 3.5 to 8.5 that of the wavelength. Therefore, the transmitted light was weak and a photon counting detector had to be used.

With the development of fiber optics, frustrated total internal reflection can be observed more easily through the tiny gap between two optical fibers,[11] or by using one optical fiber as a probe to detect the evanescent wave near the surface where total reflection occurs.[12] However, such approaches are usually too sophisticated for most undergraduate laboratories. Directly using the air gap between two prisms is a common and simple choice. Zhu *et al.*[1] conducted such an experiment with a He-Ne laser in which the gap between the prisms could be reduced to 0.2 times the wavelength. Castro[13] modified the experimental arrangement by touching the two prisms at one side, so that the air wedge between the prisms could provide a thin air film with thickness continuously changing from zero to ≈ 0.3 μm. Because the key idea is to reduce the thickness of the middle medium to the optical wavelength region, we adapted a Newton's rings apparatus to obtain the 100 nm thick air film.

II. DESIGNS AND DEVICES

A Newton's rings apparatus consists of a flat-convex lens resting on a piece of flat glass plate. There is a micrometer-wide region near the contact point in which the thickness of the air film varies continuously from zero to several hundred nanometers. The advantage of using this apparatus is that the thickness of the air film increases from zero quadratically, providing a significant area (several mm^2) in which the air film has a thickness less than the wavelength of light so that the transmitted light is strong and can be directly observed. The air film region is also small enough so that the lens faces are not required to be flat over large areas as in Castro's experiment.[13] In comparison to some previous demonstrations[1,10] where the film thickness is controlled mechanically by a micrometer screw, the film thickness here is geometrically determined by the spherical surface of the flat-convex lens and is therefore more precise.

The experimental setup is shown in Fig. 1. The light comes from a He-Ne laser. The laser beam is expanded by two lenses in the front, and is polarized to either a P or S wave. The light beam is then refracted by the prism A, so that it can reach the air film at an appropriate incident angle near the critical angle θ_c. Frustrated total reflection is ex-

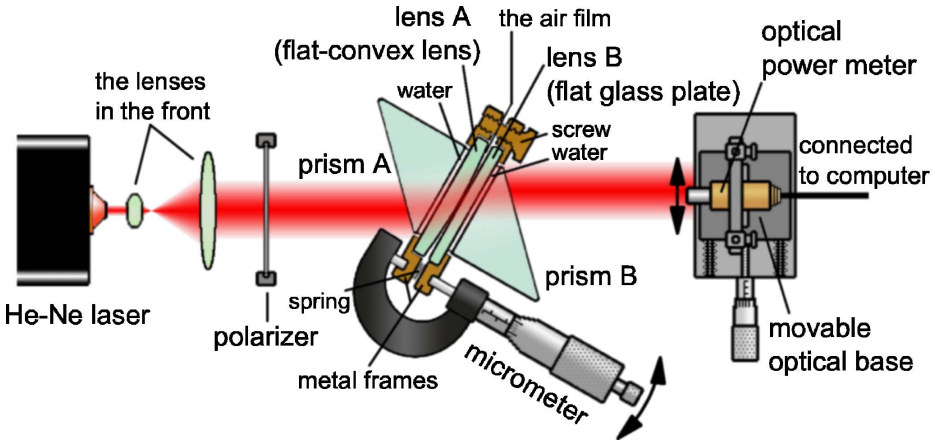

Fig. 1. (Color online) A schematic drawing of the apparatus from a bird's-eye view.

pected to occur near the center of Newton's rings. Prism B is used to direct the transmitted light out of the Newton's rings device.

Between the prisms is the Newton's rings device, which is formed by lens A (the flat-convex lens) and lens B (the flat glass plate) (see Fig. 1). Both prisms are optically connected to the lenses by introducing pure water between the interfaces. Otherwise, the light would be totally reflected before entering lens A once the incident angle exceeds the critical angle. The top seam of each interface is covered by wet cotton to prevent the water from drying during the experiment.

The double prisms and the Newton's rings device are fixed on a rotatable platform. The incident angle on the air film can be adjusted from 0° to almost 90° by rotating the platform. The incident angle was measured by a protractor equipped by a vernier on the platform with accuracy of 1′.

A paper screen can be placed behind prism B to observe the transmitted pattern. For quantitative measurements the paper screen is replaced by a linear response optical power meter (as in Fig. 1). The power meter is fixed to a horizontally movable optical base whose position can be adjusted and read from the micrometer screw near the bottom of the base.

It is crucial whether the two lenses of the Newton's rings device contact at a point or not. Losing contact or squeezing them together would lead to disagreement with the theoretical predictions given in Sec. III. We can judge the separation of the lenses by measuring the ratio of the radius of the second Newton's ring r_2 to that of the first Newton's ring r_1 (see Fig. 2). If the lenses touch at a point, the ratio should be $r_2/r_1=\sqrt{2}$ exactly.

To control and adjust the separation between the lenses A and B, one of the screws on the metal frames holding the lenses is replaced by a micrometer. A spring is placed between the metal frames to push the frames apart. Screwing the micrometer exerts pressure on the spring and reduces the spacing between the lenses. In this way, the separation of the lenses can be controlled by the micrometer to an accuracy of 0.5 μm. We adjust the micrometer and measure the ratio r_2/r_1 to ensure that its value is $\sqrt{2}\pm 0.01$, so that the two lenses are in point contact.

III. CALCULATIONS AND QUALITATIVE RESULTS

A. The transmission coefficient near the center of Newton's rings

Newton's rings results from the thin film interference of the air film lying between the lenses A and B. We now discuss how the pattern changes when the incident angle grows and exceeds the critical angle.

First consider the case of an air film with thickness d lying between two pieces of glass, whose indices of refraction are both n. If the incident angle is θ (see Fig. 3), the transmission coefficient T due to the thin film interference is given by[1]

$$T=\frac{1}{\alpha \sin^2 \xi+1}, \tag{1}$$

where ξ is a dimensionless quantity proportional to the thickness d of the air film

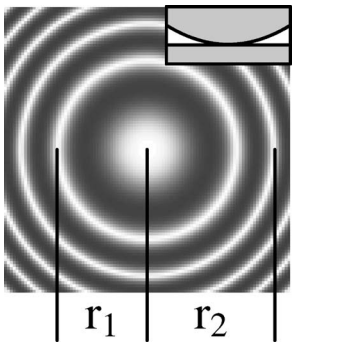

Fig. 2. The relative radii of the first two Newton's rings when lenses A and B contact at a point.

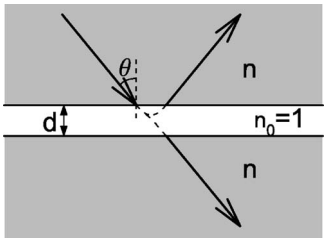

Fig. 3. A schematic diagram of frustrated total internal reflection with an air film lying between two pieces of glass.

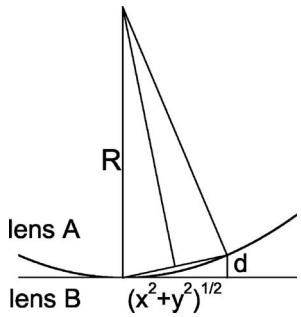

Fig. 4. The thickness d of the air film is a function of the distance $(x^2+y^2)^{1/2}$ from the (assumed single) point of contact between lenses A and B at the origin $(0,0)$.

$$\xi = \frac{2\pi d}{\lambda}(1 - n^2 \sin^2 \theta)^{1/2}. \tag{2}$$

The parameter α is related to the polarization of light. For S waves, the electric vector is perpendicular to the incident plane and

$$\alpha_S = \frac{((n^2-1)/2n)^2}{\cos^2 \theta(n^2 \sin^2 \theta - 1)}. \tag{3}$$

For P waves, the electric vector is parallel to the incident plane and

$$\alpha_P = \alpha_S((n^2+1)\sin^2 \theta - 1)^2. \tag{4}$$

Frustrated total reflection occurs when the incident angle θ exceeds the critical angle $\theta_c = \arcsin(1/n)$; that is, $\theta \geq \theta_c$. In this case ξ becomes imaginary, and $\sin^2 \xi$ should be considered as $-\sinh^2 i\xi$.

To determine the air film thickness d at each point, we set up Cartesian coordinates in the plane of the flat surface with its origin at the point of contact. Because the dimension of the first several Newton's rings (about 5 mm) is much less than the radius of curvature R of the spherical surface of lens A (roughly 2 m) (see Fig. 4), the thickness d is given approximately as by

$$d = \frac{x^2+y^2}{2R}. \tag{5}$$

We assume that the incident light is parallel, so that the incident angle θ is the same at all points. Given this assumption the entire air film shares the same value of the parameter α which can be determined by Eqs. (3) or (4). If we substitute Eq. (5) into Eq. (2), the transmission coefficient T near the center of Newton's rings is given by Eq. (1).

B. Calculation of the transmitted pattern

If the intensity of incident light is distributed uniformly, the intensity of transmitted light is proportional to the transmission coefficient T. We can numerically determine the transmitted intensities point by point. The results are plotted in Fig. 5. The calculations are performed using the experimental settings; that is, the refractive indexes of the lenses A and B are both $n=1.40$, and the critical angle is $\theta_c = \arcsin 1/1.40 = 45°35'$. The incident light is parallel and polarized to the P wave, and the lenses A and B touch at a point.

From Fig. 5 we see that the pattern of Newton's rings is a series of concentric circles resulting from the equal thickness interference. As the incident angle θ increases, the circles expand and spread out from the center [Figs. 5(a) and 5(b)]. As soon as the incident angle θ crosses over the critical angle θ_c, all the circles recede from our scope, leaving only a spot at the center of Newton's rings [Fig. 5(c)]. This spot remains there even if the incident angle has exceeded the critical angle [Fig. 5(d)].

The receding rings and the remaining spot demonstrate the phenomena of frustrated total internal reflection. When the incident angle exceeds the critical angle, total reflection occurs on the convex interface of lens A and the incident light is totally reflected, which is why all the rings spread out from the scope and disappear. Because the air film thickness near the center is of the same order as the wavelength of light, total reflection is frustrated there, and light penetrates through this part, which results in the central spot.

C. Experimental demonstration of frustrated total internal reflection

To confirm the theoretical results experimentally, a paper screen is placed behind prism B (see Fig. 1) to catch the transmitted light, and the patterns on the screen are photographed. The results are shown in Fig. 6, which are similar to the calculated patterns presented in Fig. 5. The central spot exists when the incident angle equals or exceeds the critical angle [see Figs. 6(c) and 6(d)].

Note that we have assumed that the incident light on the air film is parallel. This assumption is realized by adjusting the distance between the two lenses in the front. The thickness of the air film is symmetric with respect to the center. Due to the equal thickness interference, the transmitted pat-

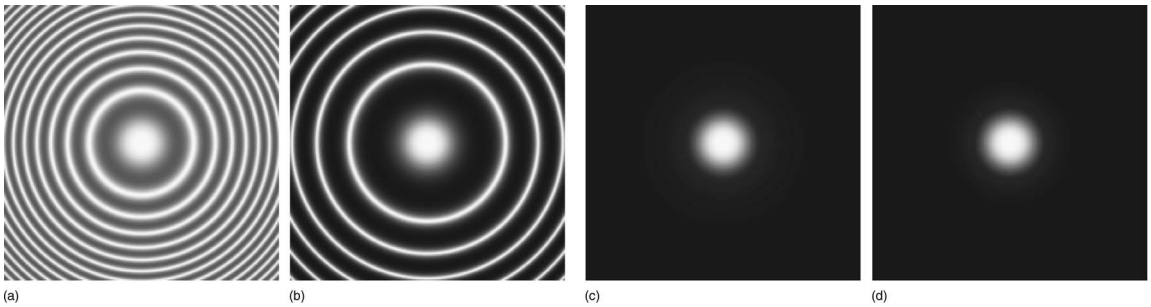

Fig. 5. Calculated intensity patterns for the transmitted light with different incident angles θ, and P wave polarization. (a) $\theta = 44°55'$, (b) $\theta = 45°27'$, (c) $\theta = 45°35' = \theta_c$, (d) $\theta = 45°43'$.

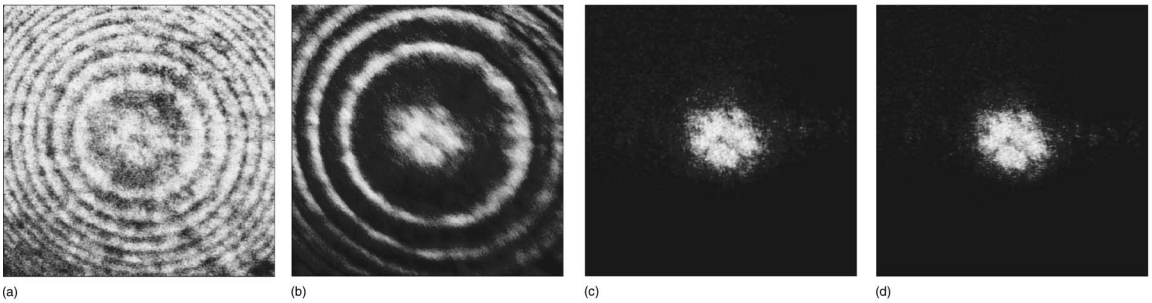

Fig. 6. Photographs of the experimentally obtained intensity patterns. The incident light is polarized as a P wave. The incident angle is adjusted to the required value by rotating the rotatable platform. (a) $\theta=44°55'$, (b) $\theta=45°27'$, (c) $\theta=45°35'=\theta_c$, (d) $\theta=45°43'$.

tern will also take the same symmetry, and hence the stripes are circular. If the incident light is not parallel, the incident angle on the air film will differ from point to point, which will lead to equal inclination interference. In this case, the circular stripes will be distorted. We adjusted the distance between the front lenses to make the stripes as circular as possible, thereby ensuring that the incident light is parallel.

IV. MEASURING AND QUANTITATIVE RESULTS

We now study the central spot quantitatively. We will show that the different behavior of P and S waves can give the refractive index n of the lenses forming the Newton's ring device.

We are interested in the central spot when the light just reaches the air film at the critical angle θ_c. In the limit that $\theta\rightarrow\theta_c$, the transmission coefficient T in Eq. (1) can be written as

$$T(x,y)=\frac{1}{b(x^2+y^2)^2+1}, \tag{6}$$

where

$$b_{\mathrm{S}}=\frac{\pi^2(n^2-1)}{4R^2\lambda^2} \quad \text{(S waves)}, \tag{7}$$

$$b_{\mathrm{P}}=\frac{\pi^2(n^2-1)}{4n^4R^2\lambda^2} \quad \text{(P waves)}. \tag{8}$$

Hence,

$$b_{\mathrm{S}}=n^4b_{\mathrm{P}}. \tag{9}$$

Because n is the refractive index of the lenses A and B, we have $n>1$. Therefore, $b_S>b_P$, which means that the size of the central spot for S wave polarization is smaller than that for P wave polarization. This phenomenon can be studied quantitatively by measuring the light intensity distribution of the central spot under different polarizations.

An optical power meter can scan along the x-axis on which the transmission coefficient T is

$$T(x,0)=\frac{1}{bx^4+1}. \tag{10}$$

In the experiment, x is read directly from the micrometer of the optical base. Therefore in the raw data the center of Newton's rings has a shift x_0 from the origin. The intensity of transmitted light can be fitted to

$$I(x,0)=\frac{I_0}{b(x-x_0)^4+1}+I_{\mathrm{BG}}, \tag{11}$$

where I_{BG} is the background light intensity of the environment, I_0 is the normalization constant of peak intensity, b denotes either b_S or b_P, and x_0 adjusts the origin of the data x to the center of Newton's rings.

Figure 7 illustrates the experimental result of the transmitted light intensity and curves fitted to Eq. (11) for the central spot. The light intensity is proportional to the voltage output of the optical power meter, which is measured in units of mV. We can see that the P wave curve is broader than that for S waves, which implies that the size of the central spot is larger for P wave polarization, in agreement with our analysis.

Fitting the data with Eq. (11) gives the values of the parameters b_{P} and b_{S}:

$$b_{\mathrm{P}}=1.16\pm0.08\ \mathrm{mm}^{-4}, \tag{12}$$

$$b_{\mathrm{S}}=4.46\pm0.23\ \mathrm{mm}^{-4}. \tag{13}$$

According to Eq. (9), the refractive index of the lenses is

$$n=\left(\frac{b_{\mathrm{S}}}{b_{\mathrm{P}}}\right)^{1/4}=1.40\pm0.04. \tag{14}$$

This result is consistent with the direct measurement result, which gives 1.40 ± 0.05 and verifies Eq. (9), and the expla-

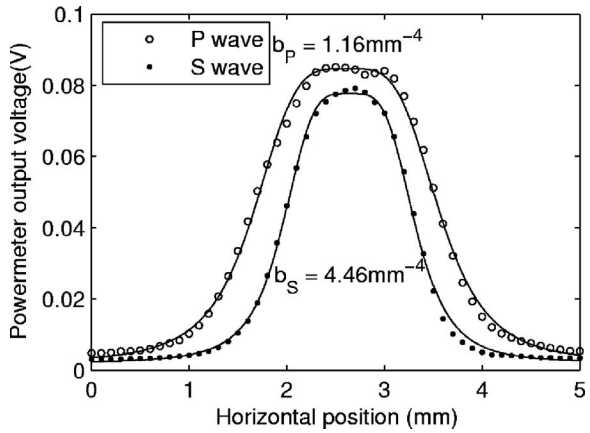

Fig. 7. Experimental distribution of the light intensity I for the central spot for P wave and S wave polarization respectively. The curves are the results of data fitting. The light intensity is proportional to the voltage output of the optical power meter, which is measured in unit of mV.

nation that the central spot result from the frustrated total internal reflection near Newton's rings.

V. CONCLUSION

Although known for hundreds of years, frustrated total internal reflection is still an intriguing phenomenon. We have devised a simple method to demonstrate this phenomenon in the visible band using a Newton's rings apparatus.

The calculations predict the existence of a light spot at the center of Newton's rings when the incident angle exceeds the critical angle, which is observed in the experiment. This central spot is a result of light tunneling through the optical barrier, and is also a direct demonstration of frustrated total internal reflection.

Theoretical calculations predict that the size of the central spot is affected by polarization of the incident light, from which we can calculate the index of refraction of the lenses forming the Newton's rings device. This prediction is quantitatively supported by experiment.

ACKNOWLEDGMENTS

The authors acknowledge the support of the Laboratory of University Physics of Nanjing University for this work. We would like to thank Z. Y. Weng for helpful suggestions.

[a]Electronic mail: everettyou@gmail.com

[1] S. Zhu, A. W. Yu, D. Hawley, and R. Roy, "Frustrated total internal reflection: A demonstration and review," Am. J. Phys. **54**, 601–607 (1986).
[2] D. W. Pohl, W. Denk, and M. Lanz, "Optical stethoscopy: Image recording with resolution $\lambda/20$," Appl. Phys. Lett. **44**, 651–653 (1984).
[3] E. Betzig, J. K. Trautman, T. D. Harris, J. S. Weiner, and R. L. Kostelak, "Breaking the diffraction barrier: Optical microscopy on a nanometric scale," Science **251**, 1468–1470 (1991).
[4] R. C. Reddick, R. J. Warmack, and T. L. Ferrell, "New form of scanning optical microscopy," Phys. Rev. B **39**, 767–770 (1989).
[5] C. Girard and A. Dereux, "Near-field optics theories," Rep. Prog. Phys. **59**, 657–699 (1996).
[6] M. Born and E. Wolf, *Principles of Optics* (Pergamon Press, Oxford, 1975), 5th ed.
[7] D. Bohm, *Quantum Theory* (Prentice Hall, Englewood Cliffs, NJ, 1951), p. 240.
[8] J. C. Bose, "On the influence of the thickness of air-space on total reflection of electric radiation," Proc. R. Soc. London **62**, 300–310 (1897).
[9] E. E. Hall, "The penetration of totally reflected light into the rarer medium," Phys. Rev. **15**, 73–106 (1902).
[10] D. D. Coon, "Counting photons in the optical barrier penetration experiment," Am. J. Phys. **34**, 240–243 (1966).
[11] K. Rahnavardy, V. Arya, A. Wang, and J. M. Weiss, "Investigation and application of the frustrated-total-internal-reflection phenomenon in optical fibers," Appl. Opt. **36**, 2183–2187 (1997).
[12] D. A. Papathanassoglou and B. Vohnsen, "Direct visualization of evanescent optical waves," Am. J. Phys. **71**, 670–677 (2003).
[13] B. C. Castro, "Optical barrier penetration–A simple experimental arrangement," Am. J. Phys. **43**, 107–108 (1975).